Desiree Wanders,[1] Laura A. Forney,[2] Kirsten P. Stone,[2] David H. Burk,[3] Alicia Pierse,[2] and Thomas W. Gettys[2]

FGF21 Mediates the Thermogenic and Insulin-Sensitizing Effects of Dietary Methionine Restriction but Not Its Effects on Hepatic Lipid Metabolism

Diabetes 2017;66:858–867 | DOI: 10.2337/db16-1212

Dietary methionine restriction (MR) produces a rapid and persistent remodeling of white adipose tissue (WAT), an increase in energy expenditure (EE), and enhancement of insulin sensitivity. Recent work established that hepatic expression of FGF21 is robustly increased by MR. *Fgf21*$^{-/-}$ mice were used to test whether FGF21 is an essential mediator of the physiological effects of dietary MR. The MR-induced increase in energy intake and EE and activation of thermogenesis in WAT and brown adipose tissue were lost in *Fgf21*$^{-/-}$ mice. However, dietary MR produced a comparable reduction in body weight and adiposity in both genotypes because of a negative effect of MR on energy intake in *Fgf21*$^{-/-}$ mice. Despite the similar loss in weight, dietary MR produced a more significant increase in in vivo insulin sensitivity in wild-type than in *Fgf21*$^{-/-}$ mice, particularly in heart and inguinal WAT. In contrast, the ability of MR to regulate lipogenic and integrated stress response genes in liver was not compromised in *Fgf21*$^{-/-}$ mice. Collectively, these findings illustrate that FGF21 is a critical mediator of the effects of dietary MR on EE, remodeling of WAT, and increased insulin sensitivity but not of its effects on hepatic gene expression.

Dietary methionine restriction (MR) produces an integrated series of metabolic and physiological responses that persistently improve biomarkers of metabolic health (1–3). The most prominent physiological responses are coordinated increases in energy intake and expenditure (2), with the larger effect on energy expenditure (EE) limiting net increases in fat deposition and accumulation of body weight (BW) (4). The MR diet also increases in vivo insulin sensitivity through a combination of direct and indirect effects on the liver, adipose tissue, and muscle (5). Although progress has been made in identifying the molecular sensors that detect MR (6–13), a full accounting of the specific mechanisms linking reduced methionine to its metabolic phenotype remains incomplete. The MR-induced improvement in insulin sensitivity is partly due to reductions in adiposity, but the MR diet also increases tissue-specific insulin sensitivity through mechanisms that are independent of differences in adiposity (4). For example, MR-dependent reductions in hepatic glutathione significantly enhance insulin signaling by slowing glutathione-dependent degradation of PIP3 (5). Dietary MR also increases secretion of the insulin sensitizer, adiponectin, from adipose tissue (2,3,14), but the ability of MR to enhance insulin sensitivity appears uncompromised in adiponectin-null mice (15).

Another promising mediator of the physiological effects of dietary MR is FGF21. Within hours of initiating dietary MR, hepatic transcription and release of FGF21 into the serum is increased by four- to fivefold (5,13). The evidence is compelling that FGF21 is a powerful metabolic regulator in the context of glucose homeostasis, lipid metabolism, and energy balance (16–22), but controversy remains about how FGF21 signaling is anatomically organized to produce its multiple physiological effects. To date, the biological responses to FGF21 have been cataloged in studies where FGF21 was infused at high doses or increased via transgenic overexpression, so whether the physiological increases produced by MR are sufficient to

[1]Department of Nutrition, Georgia State University, Atlanta, GA
[2]Laboratory of Nutrient Sensing and Adipocyte Signaling, Pennington Biomedical Research Center, Baton Rouge, LA
[3]Cell Biology & Bioimaging Core, Pennington Biomedical Research Center, Baton Rouge, LA

Corresponding author: Thomas W. Gettys, thomas.gettys@pbrc.edu.

Received 5 October 2016 and accepted 10 January 2017.

D.W. and L.A.F. contributed equally to this work.

elicit all of the responses produced by pharmacological modulation of FGF21 is unclear (23). However, many if not most of the metabolic, transcriptional, and signaling effects attributed to FGF21 are fully reproduced by dietary MR (1,2,4,5,24). Using *Fgf21*$^{-/-}$ mice and dietary MR in both low-fat and high-fat (HF) contexts, we report here that FGF21 is an essential mediator of the effects of MR on EE and energy intake but not overall energy balance due to a paradoxical decrease in intake of the MR diet in *Fgf21*$^{-/-}$ mice. The greater enhancement of insulin sensitivity by MR in wild-type (WT) versus *Fgf21*$^{-/-}$ mice, despite a comparable loss of BW, suggests a partial but significant FGF21-dependent role in the mechanism. In contrast, the expected transcriptional responses to MR in the liver are fully intact in *Fgf21*$^{-/-}$ mice, supporting a FGF21-independent mechanism of action.

RESEARCH DESIGN AND METHODS

The vertebrate animal experiments in this study were reviewed and approved by the Pennington Institutional Animal Care and Use Committee using guidelines established by the National Research Council, the Animal Welfare Act, and the Public Health Service Policy on humane care and use of animals.

Animals and Diets

Fgf21$^{-/-}$ mice on the C57BL/6J genetic background were provided by Dr. Steven Kliewer (UT Southwestern). Two different dietary formulations of the control (CON) and MR diets, differing in energy density, were manufactured by Dyets Inc. (Bethlehem, PA). The energy content of the CON (Dyets #510072) and MR diets (Dyets #510071) used in experiments 1–3 was 15.96 kJ/g, with 18.9% of energy from fat (corn oil), 64.9% from carbohydrate, and 14.8% from a custom mixture of L-amino acids. The amino acid content of the diets on a weight basis was 14.1%. The CON diet contained 0.86% methionine, and the MR diet contained 0.17% methionine. For experiment 4, the energy density of the CON and MR diets was increased to 22.8 kJ/g, with 59.6% of energy from fat (lard and soybean oil), 25.7% from carbohydrate, and 14.7% from L-amino acids. The HF CON diet contained 0.86% methionine, and the HF MR diet contained 0.17% methionine. Food and water were provided ad libitum, and lights were on 12 h/day from 7 A.M. to 7 P.M. Mice were euthanized by CO_2 narcosis, followed by decapitation.

Experiment 1

Five-week-old male WT (n = 16) and *Fgf21*$^{-/-}$ (n = 16) C57BL/6J mice were acclimated to the CON diet for 1 week before the mice were adapted to the TSE Indirect Calorimetry system. All mice received the CON diet during the adaptation period. Thereafter, eight mice of each genotype were switched to the MR diet and eight mice of each genotype continued on the CON diet. VO_2 and VCO_2 were measured at 40-min intervals for an additional 11–12 days. The respiratory quotient (RQ) was calculated as the ratio of VCO_2 produced to VO_2 consumed. EE was calculated as (VO_2*[3.815 + {1.232*RQ}]*4.1868).

Experiment 2

Five-week old male WT (n = 20) and *Fgf21*$^{-/-}$ (n = 20) C57BL/6J mice were acclimated to the CON diet for 1 week, and then half the mice of each genotype were switched to the MR diet while the other half continued on the CON diet. Food intake, BW, and composition were measured weekly for 9 weeks before all mice were adapted to the TSE system for 2 days, followed by measurement of VO_2, VCO_2, activity, and food intake at 40-min intervals for 3 days. Mice were euthanized 1 week later, and tissues were harvested after a 4-h fast. Group differences in EE (kJ/mouse/h) were compared using ANCOVA (JMP Statistical Software, version 11; SAS Institute Inc., Cary, NC), calculating least squares means that accounted for variation in EE attributable to differences in lean mass, fat mass, activity, energy intake, genotype, diet, and genotype × diet interaction (4). The least squares means ± SEM for the genotype × diet combinations were compared using a two-way ANOVA, and the significance of the model effects and interaction were tested using residual variance calculated by ANCOVA.

Experiment 3

A third cohort of WT (n = 20) and *Fgf21*$^{-/-}$ (n = 20) mice was shipped to the Vanderbilt Phenotyping Center at 5 weeks of age to undergo hyperinsulinemic-euglycemic clamps as previously described (5,25). Mice of each genotype were fed the CON diet for 3 weeks before being randomized to the CON or MR diet for the following 13 weeks before surgery for catheter placement. After a 5-day recovery, clamps were performed in conscious mice after a 5-h fast. Insulin (2.5 mU/kg/min) was infused with a 50% dextrose solution at a variable rate to maintain euglycemia. Whole-body glucose turnover was assessed with a 5 μCi bolus of [3-^{3}H]glucose tracer 1.5 h before insulin treatment, followed by a 0.05 μCi/min infusion during the clamp. Insulin-stimulated glucose uptake in individual organs was determined using 2-[^{14}C]deoxyglucose ([^{14}C]2-DG) administered as a single bolus (13 μCi) 120 min after the start of clamp procedure. At t = 145 min, epididymal WAT, inguinal WAT (IWAT), brown adipose tissue (BAT), gastrocnemius muscle, vastus lateralis muscle, soleus muscle, brain, and heart were harvested for analysis. Steady-state glucose infusion rates (GIRs), glucose levels, plasma insulin, BWs, and R_g in each tissue were compared by two-way ANOVA.

Experiment 4

Male WT (n = 24) and *Fgf21*$^{-/-}$ (n = 24) C57BL/6J mice (12 weeks old) were acclimated to the HF CON diet for 4 weeks before half of the mice of each genotype were switched to the HF MR diet. Food intake, BW, and composition were measured weekly for 8 weeks. After a 2-week recovery, mice were adapted to TSE system for 2 days, followed by measurement of VO_2, VCO_2, activity, and food intake at 40-min intervals for 3 days. Data were analyzed

as described for experiment 2. Tissues and serum were harvested 1 week after indirect calorimetry after a 4-h fast.

Western Blotting

Expression of fatty acid synthase (FASN), and stearyl-CoA desaturase (SCD-1) were measured by Western blotting as previously described (1). The FASN antibody was from Santa Cruz (Dallas, TX), the β-actin antibody was from Sigma-Aldrich (St. Louis, MO), and the affinity-purified SCD-1 antibody was described previously (1). Detected proteins were quantitated using ImageJ software, and the relative expression of the target protein versus β-actin was calculated to test for genotype and diet effects.

RNA Isolation and Quantitative Real-Time PCR

Total RNA was isolated using an RNeasy Mini Kit (QIAGEN Inc., Valencia, CA). One microgram of total RNA was reverse transcribed to produce cDNA. Gene expression was measured by real-time PCR (Applied Biosystems, Foster City, CA) by measurement of SYBR Green. mRNA concentrations were normalized to cyclophilin expression.

Histology

Paraffin-embedded IWAT tissues from experiment 1 were sectioned at 5 μm and stained for hematoxylin and eosin as previously described (26).

Liver and Serum Triglyceride

Serum and lipid triglyceride levels were measured as previously described (2).

RESULTS

Role of FGF21 in MR-Induced Effects on EE and Energy Balance

Comparison of the acute effects of dietary MR on EE in WT and *Fgf21*$^{-/-}$ mice showed that the diet significantly increased EE at day 6 in WT mice and expanded the magnitude of the effect over the subsequent 6 days (Fig. 1*A*). In

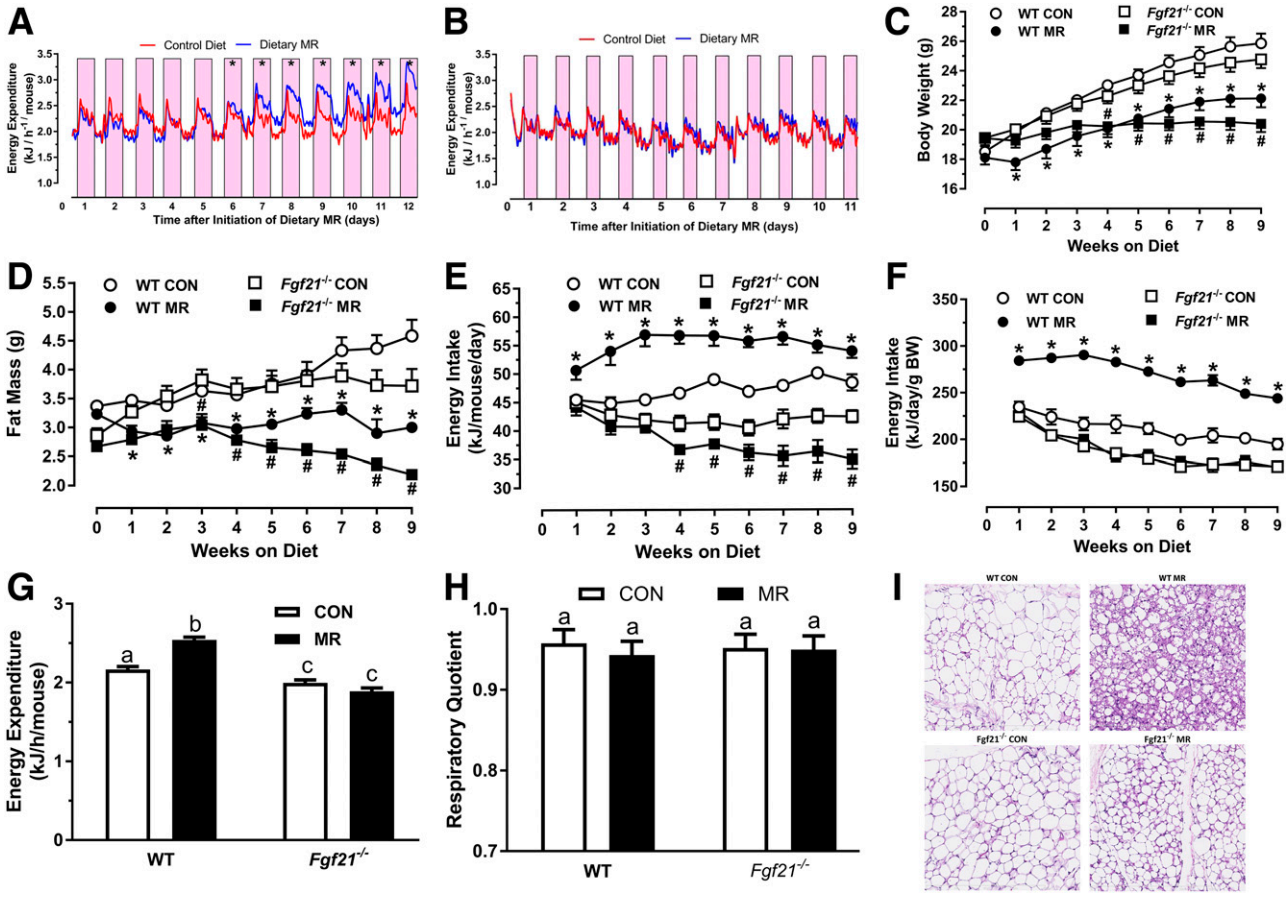

Figure 1—Assessment of acute and chronic effects of dietary MR on EE and energy balance in WT and *Fgf21*$^{-/-}$ mice. EE was measured by indirect calorimetry in WT (*A*) and *Fgf21*$^{-/-}$ mice (*B*). Mice fed the CON diet were placed in the TSE calorimeters and were randomized to remain on CON or switched to MR while in the TSE. The effect of diet on 24-h EE was compared for each day within genotype during the following 11 days. Days annotated with an * differ from mice fed the CON diet at $P < 0.05$. Change in BW (*C*), fat mass (*D*), energy intake per mouse (*E*), and energy intake per unit BW (*F*) for 9 weeks in WT and *Fgf21*$^{-/-}$ mice after initiation of dietary MR. Means ± SEM are presented for weekly measurements in 8 mice per diet per genotype, and means annotated with * and # differ from mice of the same genotype fed the CON diet at $P < 0.05$. Least squares means ± SEM of EE (*G*) and RQ (*H*) determined after 9 weeks on respective diets and measured over 3 days in eight mice per diet per genotype. Least squares means of EE were calculated by ANCOVA as described in RESEARCH DESIGN AND METHODS. EE and RQ were compared by a two-way ANOVA. Means annotated with a different letter (a, b, c) differ at $P < 0.05$. *I*: Hematoxylin and eosin stains of representative sections of IWAT from WT and *Fgf21*$^{-/-}$ mice fed the CON or MR diet for 9 weeks.

contrast, dietary MR had no effect on EE in *Fgf21*$^{-/-}$ mice in the first 11 days the diet was provided (Fig. 1*B*), supporting the view that FGF21 is required for the acute increase in EE produced by MR.

BW of WT and *Fgf21*$^{-/-}$ mice fed the CON diet did not differ at the beginning of experiment 2, but BW diverged slightly over the final 5 weeks, with WT mice ending the study slightly but not significantly heavier than *Fgf21*$^{-/-}$ mice (Fig. 1*C*). In WT and *Fgf21*$^{-/-}$ mice fed the CON diet, the change in fat mass over time paralleled the change in BW (Fig. 1*D*). This difference in BW in mice fed the CON diet is reflected in the slightly but not significantly higher energy intake in WT mice compared with *Fgf21*$^{-/-}$ mice (Fig. 1*E*). Dietary MR produced a significant increase in energy intake in WT mice during the entire study (Fig. 1*E*), but their accumulation of BW and fat mass was significantly lower than WT mice fed the CON diet (Fig. 1*C* and *D*). In contrast, MR decreased energy intake in *Fgf21*$^{-/-}$ mice after 4 weeks, and the decrease translated into reduced accumulation of BW and fat mass in *Fgf21*$^{-/-}$ mice fed the MR diet (Fig. 1*C* and *D*). However, the identical energy intake per unit BW of *Fgf21*$^{-/-}$ mice fed the respective diets indicates that the loss in BW and fat mass of *Fgf21*$^{-/-}$ mice fed the MR diet is accounted for by their reduction in intake per mouse (Fig. 1*E* and *F*). The primary effect of MR on body composition in both genotypes was to reduce fat deposition (Fig. 1*D*), but the mechanism in WT mice was an increase in EE (Fig. 1*A* and *G*), whereas the mechanism in *Fgf21*$^{-/-}$ mice was reduced energy intake (Fig. 1*E*). The indirect calorimetry conducted at the end of the study showed that MR significantly increased EE in WT mice but was without effect in *Fgf21*$^{-/-}$ mice (Fig. 1*G*). Dietary MR failed to reduce RQ in either genotype, and the RQs were similar across genotypes within the diet (Fig. 1*H*). The appearance of WAT was also differentially affected by MR between the genotypes, with MR producing the previously shown remodeling of cell and fat droplet morphology in the inguinal depot (4,27) of WT mice and only a modest reduction in adipocyte size in *Fgf21*$^{-/-}$ mice (Fig. 1*I*). Together, these findings illustrate that FGF21 is an essential mediator of the effects of dietary MR on energy intake, EE, and remodeling of WAT.

Role of FGF21 in MR-Induced Effects on Insulin Sensitivity

We previously showed that dietary MR for 8–10 weeks produces a two- to threefold increase in overall insulin sensitivity (5,13). To test whether FGF21 was an essential mediator of this effect, hyperinsulinemic-euglycemic clamps were used to assess insulin sensitivity in WT and *Fgf21*$^{-/-}$ mice. The GIRs needed to establish euglycemia after the insulin infusion was initiated were comparable between WT and *Fgf21*$^{-/-}$ mice fed the CON diet, and MR produced a significant increase in steady-state GIR between 80 to 120 min in both genotypes (Fig. 2*A*). The steady-state levels of blood glucose during the clamp were comparable among the groups (Fig. 2*B*), as were plasma insulin levels before and during the clamp (Fig. 2*C*). The MR-dependent increase in GIR in WT mice was nearly threefold, whereas the increase in *Fgf21*$^{-/-}$ mice was approximately twofold (Fig. 2*A*). MR produced a comparable reduction in BW in this study (Fig. 2*D*) and a slightly greater reduction in fat mass in experiment 2 (Fig. 1*D*). Thus, the slightly greater improvement in overall insulin sensitivity produced by MR in WT compared with *Fgf21*$^{-/-}$ mice suggests a body size– or composition-independent component of the improvement in insulin sensitivity that is FGF21 dependent (Fig. 2*A*). The R_g provides a measure of insulin-dependent plus -independent glucose uptake and showed that MR enhanced [^{14}C]2-DG uptake by two- to threefold in gastrocnemius muscle, vastus lateralis muscle, soleus muscle, and heart in WT mice (Fig. 2*E* and *F*). In contrast, the MR-dependent increase in skeletal muscle R_g in *Fgf21*$^{-/-}$ mice was intermediate in that it did not differ from *Fgf21*$^{-/-}$ mice fed the CON diet or WT mice fed the MR diet (Fig. 2*E*). In the heart, MR had no detectable effect on R_g in *Fgf21*$^{-/-}$ mice (Fig. 2*F*). MR did increase R_g by fourfold in IWAT of *Fgf21*$^{-/-}$ mice, whereas the increase in WT mice was ninefold, indicating a more significant effect of MR when FGF21 was present (Fig. 2*G*). Together, these data provide compelling evidence that FGF21 is an essential mediator of the insulin-sensitizing effects of MR, working through both weight-dependent and -independent mechanisms.

Role of FGF21 in Reversal of Diet-Induced Obesity by Dietary MR

After WT and *Fgf21*$^{-/-}$ mice were adapted to the HF CON diet for 4 weeks, initiation of the HF MR diet produced an immediate and comparable reversal of BW (Fig. 3*A*) and fat accumulation (Fig. 3*B*) in both genotypes. During this first 4-week period, BW and fat mass decreased in parallel in each genotype and remained essentially constant during the last 4 weeks of the study (Fig. 3*A* and *B*). By comparison, the BW and fat mass of WT and *Fgf21*$^{-/-}$ mice fed the HF CON diet steadily increased during the 8-week study (Fig. 3*A* and *B*). The 40% reduction in BW of WT mice fed the HF MR diet versus the HF CON diet occurred despite a 30% higher rate of energy intake in WT mice fed the HF MR diet compared with the HF CON diet (Fig. 3*C*). Even after energy intake was adjusted to the difference in BW, WT mice fed the HF MR diet were still consuming significantly more than WT mice fed the HF CON diet (Fig. 3*D*), indicative of a higher rate of EE. In contrast, the rapid and significant loss of BW in *Fgf21*$^{-/-}$ mice fed the HF MR diet is entirely attributable to a reduction in energy intake that becomes evident after 2 weeks and persists for 4 of the 8 weeks of the study (Fig. 3*C*). Measurements of EE after 9 weeks on the respective diets support this conclusion and show that MR produced a significant increase in EE in WT but not *Fgf21*$^{-/-}$ mice (Fig. 3*E*). The HF configurations of the CON and MR diets reduced RQs to ~0.8 in all groups, and no genotype, diet,

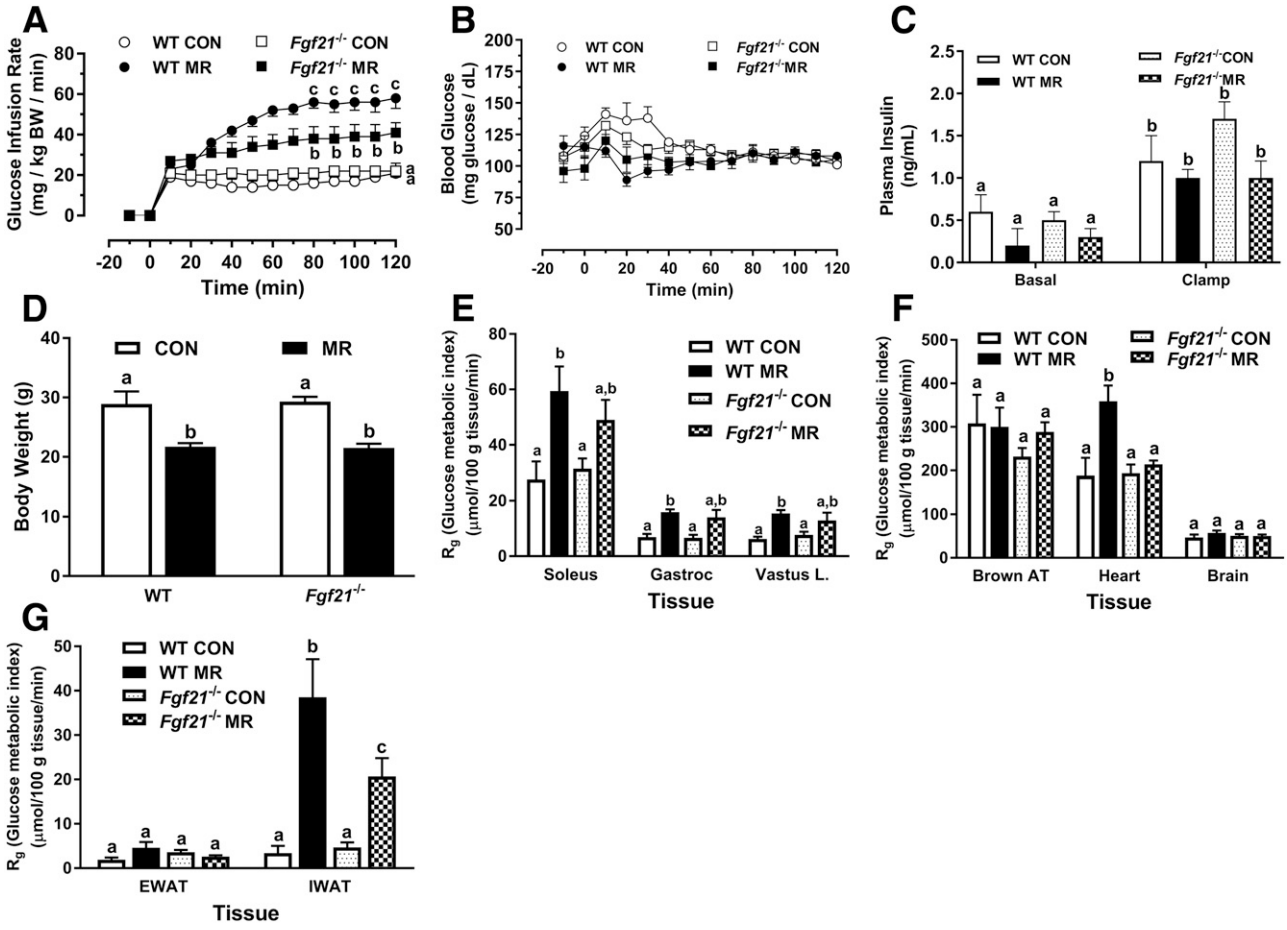

Figure 2—Hyperinsulinemic-euglycemic clamps in WT and *Fgf21*$^{-/-}$ mice after 13 weeks of dietary MR to test for effects on overall insulin sensitivity and insulin-dependent 2-DG uptake among tissues. The clamp procedures were conducted as described in RESEARCH DESIGN AND METHODS. *A*: The GIR required to maintain euglycemia during the insulin clamps is shown. Blood glucose concentration (*B*) and plasma insulin concentration (*C*) are shown before and during the insulin clamps. *D*: The effect of the CON and MR diets on the respective BWs of WT and *Fgf21*$^{-/-}$ mice is shown. R_g is shown for skeletal muscle (*E*); BAT, heart, and brain (*F*); and epididymal WAT (EWAT) and IWAT (*G*). R_g provides a measure of insulin-dependent plus insulin-independent glucose uptake in each tissue. The R_g for each tissue were compared by two-way ANOVA and means ± SEM are based on n = 7–9 mice per genotype and diet. Means annotated with different letters (a, b, c) within each tissue differ at $P < 0.05$.

or genotype × diet interactions were detected (Fig. 3*F*). Thus, in both low-fat and HF contexts, FGF21 appears to be an essential mediator of MR's effect on energy intake and EE.

Role of FGF21 as a Mediator of Transcriptional Effects of Dietary MR in the Liver

To examine the role of FGF21 as a mediator of the transcriptional effects of MR in the liver, previously identified targets of MR were measured in mice from experiment 4. For example, previous studies identified lipogenic genes as targets and showed that MR produced a coordinated downregulation of these genes (1). Examination of the key genes involved in hepatic de novo lipogenesis (e.g., *Scd1, Fasn, Acc1*) in WT and *Fgf21*$^{-/-}$ mice showed that the HF MR diet reduced *Scd1* mRNA expression by ~10-fold and *Fasn* mRNA by ~2-fold in WT and *Fgf21*$^{-/-}$ mice (Fig. 4*A*). The reduction in hepatic *Acc1* mRNA by MR was not significant in either genotype. Dietary MR also produced comparable reductions in SCD-1 (Fig. 4*B*) and FASN (Fig. 4*C*) protein expression in both genotypes. Hepatic triglyceride levels were reduced by twofold by MR in WT mice and were accompanied by a significant decrease in serum triglycerides (Fig. 4*D*). MR produced a larger threefold reduction in hepatic triglycerides in *Fgf21*$^{-/-}$ mice but had no effect on serum triglycerides. We recently showed that MR regulated the integrated stress response in liver by activation of NRF2 and ATF4 (13). Figure 4*E* shows that the transcriptional activation of genes from these pathways was comparable between WT and *Fgf21*$^{-/-}$ mice. Together, these findings support the view that FGF21 is not required for MR-dependent regulation of lipogenic, NRF2-dependent, or ATF4-dependent genes in the liver.

Role of FGF21 as a Mediator of Transcriptional Effects of Dietary MR in Adipose Tissue

Consumption of a MR diet induces significant browning of WAT and activation of thermogenesis in BAT (2,4,14,27). The MR diet also remodels WAT lipid metabolism by upregulating lipogenic gene expression (1). To explore the role of FGF21 in MR-dependent transcriptional responses in BAT

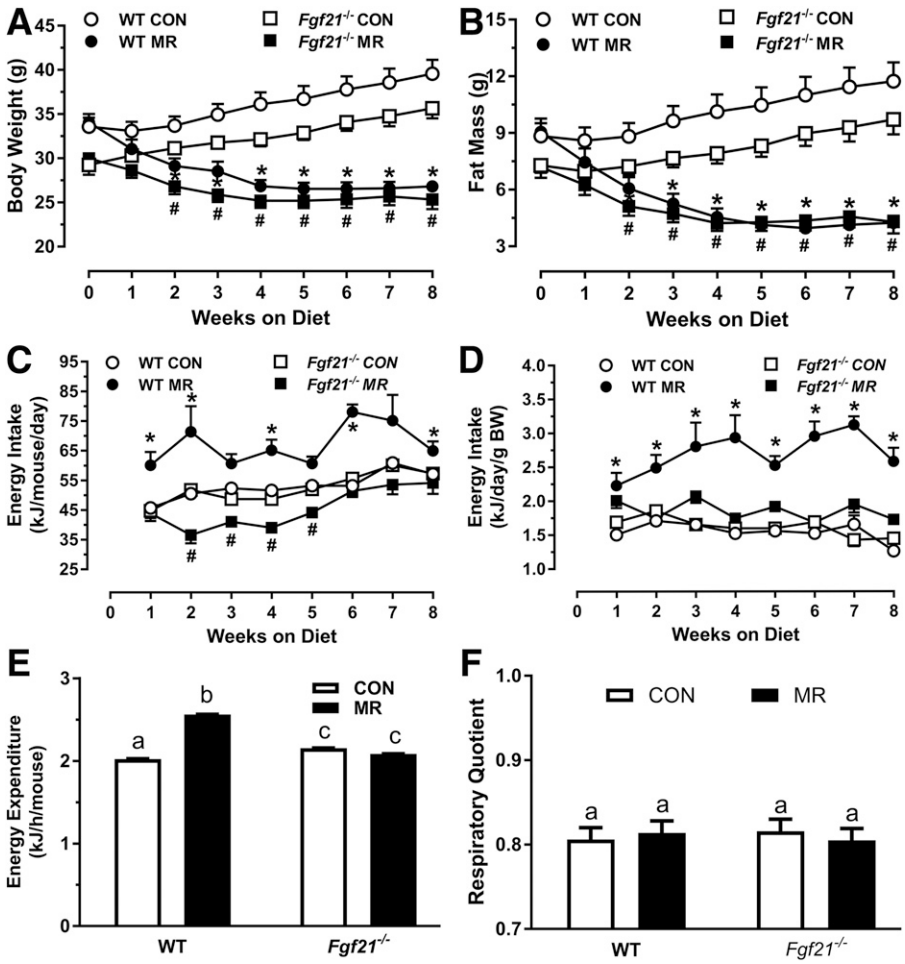

Figure 3—Assessment of chronic effects of HF CON and HF dietary MR on energy balance and EE in WT and *Fgf21*$^{-/-}$ mice. WT and *Fgf21*$^{-/-}$ mice (12 weeks old) were fed the HF CON diet for 4 weeks before half of the mice of each genotype were randomized to remain on the HF CON diet and the remaining half of mice were switched to the HF MR diet. Change in BW (*A*), fat mass (*B*), energy intake per mouse (*C*), and energy intake per unit BW (*D*) for 8 weeks in WT and *Fgf21*$^{-/-}$ mice after initiation of dietary MR. Means ± SEM are presented for weekly measurements in 10 mice per diet per genotype. Means annotated with symbols (*, #) differ from mice of the same genotype fed the CON diet at $P < 0.05$. Least squares means ± SEM of EE (*E*) and RQ (*F*) determined after 8 weeks on respective diets and measured over 3 days in eight mice per diet per genotype (*E*). Means annotated with a different letter (a, b, and c) differ at $P < 0.05$.

and WAT, we measured transcriptional markers of thermogenesis in BAT and lipogenesis and browning in IWAT from each genotype of experiment 4. In WT mice, the HF MR diet produced significant increases in markers of thermogenesis (*Ucp1, Bmp8b, Cidea, Elov3*) in BAT (Fig. 5*A*), lipogenesis (*Scd1, Fasn, Acc1, Elovl6*) in IWAT (Fig. 5*B*), and thermogenic remodeling (*Ucp1, Cox7a1, Cox8b, Cidea*) in IWAT (Fig. 5*C*). In contrast, with the exception of a positive effect on *Acc1* in IWAT, the MR diet was ineffective in inducing the thermogenic or lipogenic programs in BAT and WAT of *Fgf21*$^{-/-}$ mice (Fig. 5*A–C*). Together these findings illustrate that FGF21 is an essential mediator of the transcriptional programs induced by dietary MR in BAT and WAT.

DISCUSSION

Dietary MR produces a coordinated series of biochemical and physiological responses that develop soon after initiation of MR and persist for as long as the diet is consumed (3,14,28–31). The biological significance of these effects in aggregate is substantial, resulting in animals that are leaner, more insulin sensitive, and live longer (1,2,24,32,33). The most significant unanswered questions pertain to how the reduction in dietary methionine is sensed and how these sensing mechanisms are coupled to tissue-specific responses that produce the resulting metabolic phenotype. Previous studies establish that dietary MR produces a rapid, robust, and persistent increase in hepatic transcription and release of FGF21 (4,5,15,34). The evidence is also compelling that FGF21 is a powerful metabolic regulator in the context of glucose homeostasis, lipid metabolism, and energy balance (16–22), but controversy remains about how FGF21 signaling is anatomically organized to produce its multiple physiological effects. The biological responses to FGF21 have been documented in studies where FGF21 was infused at high doses or increased via transgenic overexpression, so it

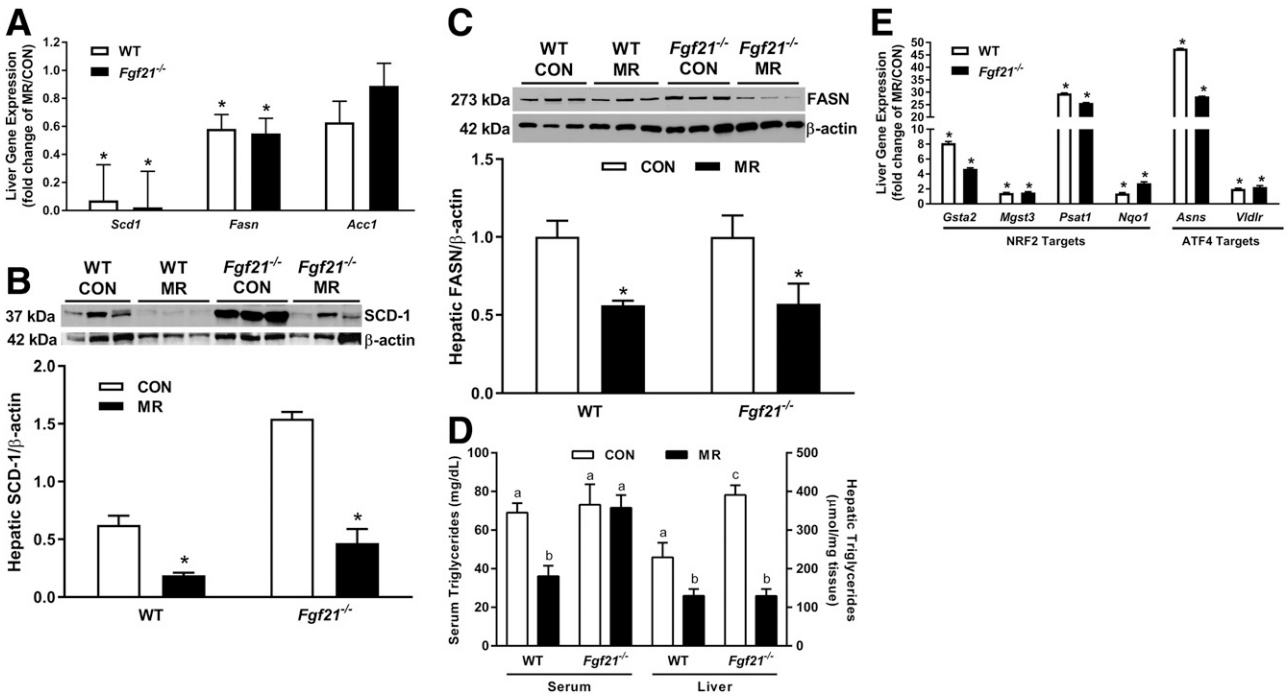

Figure 4—Effects of HF CON and HF dietary MR on hepatic gene expression and on liver and serum triglycerides in WT and *Fgf21*$^{-/-}$ mice. WT and *Fgf21*$^{-/-}$ mice (12 weeks old) were fed the HF CON diet for 4 weeks before half the mice of each genotype were randomized to remain on the HF CON diet and the remaining half of mice were switched to the HF MR diet for 8 weeks. Effects of MR on hepatic lipogenic gene expression (*A* and *B*) or NRF2-sensitive and ATF4-sensitive gene expression (*E*) were expressed as fold change in the MR group/CON group within genotype for each gene (*A* and *E*). The respective mRNAs were measured by real-time PCR. Expression of SCD-1 (*B*) and FASN (*C*) was determined in representative liver microsomes for SCD-1 and cytosol for FASN in mice from each genotype and diet. Expression of SCD-1 and FASN were expressed relative to β-actin. *D*: Serum and liver triglycerides were measured as described in RESEARCH DESIGN AND METHODS. Means in panel *D* that are annotated with different letters (a, b, c) within tissue differ at $P < 0.05$ ($n = 10$/group). Fold-changes in expression for each gene in panels *A* and *E* are representative of 10 mice per diet per genotype. Means annotated with an * differ from the CON diet within genotype at $P < 0.05$.

is unclear whether the physiological increases produced by MR (e.g., 1 ng/mL to 8 ng/mL [13]) are sufficient to elicit all of the responses produced by pharmacological modulation of FGF21 (23). Many of the metabolic, transcriptional, and signaling effects attributed to FGF21 are fully reproduced by dietary MR (1,2,4,5,24). For example, FGF21 directly affects adiponectin secretion from adipocytes (35), increases lipogenic gene expression in WAT (16), promotes browning of WAT (36), and increases thermogenic gene expression in BAT and WAT (36). Dietary MR produces significant browning of WAT (1,2,27), and given the increased glucose uptake and utilization associated with browning (37), the suggestion that MR is functioning through this mechanism to increase insulin sensitivity in WAT is attractive. However, recent reports argue that the glycemic improvements produced by FGF21 are independent of browning in WAT (38, 39) and are dependent on direct effects of FGF21 in adipose tissue (5,18,40,41). This view is also supported by studies showing that pegylated FGF21, which is too large to penetrate the central nervous system (CNS), is fully effective in normalizing glucose utilization in insulin-resistant states (42). However, from the findings presented here, it seems clear that MR-dependent increases in FGF21 affect tissue-specific and overall insulin sensitivity through a combination of mechanisms involving both decreased adiposity and direct effects of FGF21 in specific tissues.

Our previous work focused on liver and adipose tissue not only as primary transcriptional targets of dietary MR (1,24) but also as key sites for the insulin-sensitizing effects of the diet (5,13). The current study provides intriguing new observations supporting the view that *1*) the heart is an important target for the enhancement of insulin-dependent glucose uptake by dietary MR and that *2*) FGF21 is required for the MR-dependent enhancement of cardiac glucose uptake (Fig. 2*F*). Given the contribution of the heart to whole-body glucose disposal in the mouse, it seems likely that the MR-dependent increase in FGF21 plays a key role in enhancing overall insulin-dependent glucose utilization through its effects on cardiac glucose uptake. Pharmacological administration of FGF21 was also shown to increase glucose uptake in the heart (22), but the present observations are the first to our knowledge of physiologically relevant alterations of FGF21 enhancing insulin-dependent glucose uptake in the heart. Mice lacking the intestinal and renal neutral amino acid transporter (e.g., Slc6a19) that transports dietary methionine into the enterocyte have impaired absorption of dietary

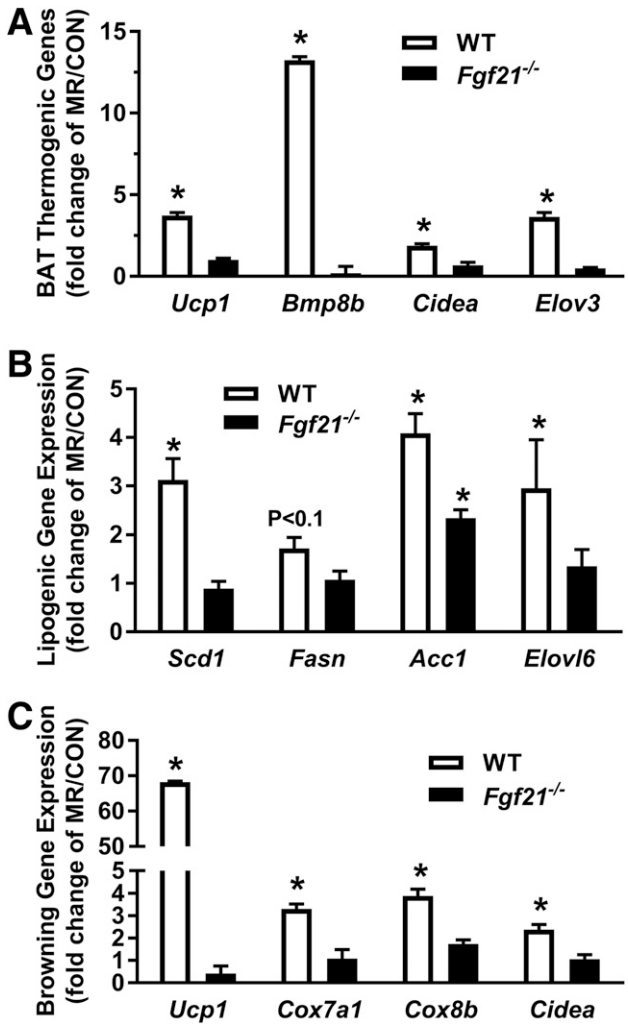

Figure 5—Effects of HF CON and HF dietary MR on gene expression in BAT and WAT from WT and *Fgf21*$^{-/-}$ mice. WT and *Fgf21*$^{-/-}$ mice (12 weeks old) were fed the HF CON diet for 4 weeks before half of the mice of each genotype were randomized to remain on the HF CON diet and the remaining half of mice were switched to the HF MR diet for 8 weeks. Effects of MR on thermogenic gene expression in BAT (*A*), lipogenic gene expression in IWAT (*B*), and browning genes in IWAT (*C*) were expressed as fold change in the MR group/CON group within genotype for mRNA levels for each gene and tissue. The respective mRNAs were measured by real-time PCR, and the means are representative of 10 mice per diet per genotype. Means annotated with an * differ from the CON diet within genotype at $P < 0.05$.

methionine and increased methionine excretion (43). Interestingly, *Slc6a19*$^{-/-}$ mice have elevated circulating FGF21 concentrations and enhanced glucose uptake, especially in the heart (44). In contrast, liver-specific deletion of FGF21 does not seem to affect glucose uptake by the heart (45). Considered together, the present findings make a compelling case that the heart is an important metabolic target of dietary MR by virtue of MR's enhancement of hepatic transcription and release of FGF21. In addition to direct effects in peripheral tissues, FGF21 also acts centrally. Although all of the CNS sites where FGF21 is acting remain ill defined, FGF21 affects EE through an increase in sympathetic nervous system outflow to adipose tissue (21,35,46,47). Dietary MR increases core temperature, EE, and thermogenic function in BAT and WAT through increases in sympathetic nervous system stimulation of adipose tissue (2,14). Our present findings make a compelling case that the MR-dependent increase in hepatic FGF21 is the key event linking MR to its metabolic effects on EE through remodeling of adipose tissue and enhanced thermogenic capacity. Sorting out the relative contributions of peripheral versus central FGF21 signaling during MR will require careful phenotyping of loss of MR-dependent effects after selective deletion of FGF21 signaling in the respective sites.

Comparisons of energy balance of WT and *Fgf21*$^{-/-}$ mice fed CON diets are also important in interpreting the present findings. In mice fed the low-fat CON diet, BWs of *Fgf21*$^{-/-}$ mice trended lower by the end of the study, and this was likely the product of slightly lower energy intakes and EE in *Fgf21*$^{-/-}$ compared with WT mice (Fig. 1*C*, *E*, and *G*). This finding differs slightly from our earlier finding of similar EE in WT and *Fgf21*$^{-/-}$ mice (13) but agrees with previous reports of lower EE in *Fgf21*$^{-/-}$ compared with WT mice (48, 49). In contrast, BWs were lower in *Fgf21*$^{-/-}$ than WT mice after 12 weeks on the HF CON diet (Fig. 3*A*), and this occurred despite similar intake of the HF CON diet during the study (Fig. 3*C*). Interestingly, EE in *Fgf21*$^{-/-}$ mice fed the HF CON diet was 6.4% higher than WT mice (Fig. 3*E*), suggesting that the higher EE at equivalent energy intake may have translated into reductions of BWs in *Fgf21*$^{-/-}$ mice. Previous reports have detected no differences in BWs between WT and *Fgf21*$^{-/-}$ mice fed HF diets (50,51), although the mice in those studies were somewhat older than the mice used in this study.

The most surprising finding from the present work is that *Fgf21*$^{-/-}$ mice fed the MR diet lost as much BW and adiposity as WT mice. However, careful examination of the data (Figs. 1 and 3) illustrates that MR affected weight and adiposity in WT and *Fgf21*$^{-/-}$ mice through completely different mechanisms. For example, despite increasing energy intake and EE in WT mice, the MR diet limited adipose tissue accretion because of its proportionately larger effect on EE. In contrast, the MR diet had no effect on EE in *Fgf21*$^{-/-}$ mice and actually reduced their energy intake to levels below that of *Fgf21*$^{-/-}$ mice fed the CON diet (Figs. 1*E* and 3*C*). This translated into comparable negative energy balances between WT and *Fgf21*$^{-/-}$ mice fed the MR diet. A further illustration that the weight loss of *Fgf21*$^{-/-}$ mice fed the MR diet is exactly proportional to their decrease in intake is obtained by expressing energy intake per unit BW. Figures 1*E* and 3*D* show that the decreased weight gain in *Fgf21*$^{-/-}$ mice fed the MR diet, relative to *Fgf21*$^{-/-}$ mice fed the CON diet, is exactly proportional to their decrease in intake. This interpretation assumes that MR is not altering EE in *Fgf21*$^{-/-}$ mice fed the MR diet, which was confirmed by independent measurements of EE in these mice.

The mechanism underlying the negative effect of MR on energy intake in *Fgf21*$^{-/-}$ mice is unknown. Low-protein (LP) diets recapitulate the effects of MR on hepatic release

of FGF21, increased energy intake, and increased EE in WT mice, but recent work showed that the LP diet did not produce hypophagia in *Fgf21*$^{-/-}$ mice (52). Because of this neutral effect on food intake, *Fgf21*$^{-/-}$ mice fed the LP diet grew at the same rate as WT mice fed the CON diet (52). A negative effect of MR on energy intake was also observed in *Ucp1*$^{-/-}$ mice, where the MR diet also failed to increase EE (4). Thus, a common feature of MR's inability to increase EE in *Fgf21*$^{-/-}$ and *Ucp1*$^{-/-}$ mice was the negative effect of the MR diet on energy intake. One interpretation of these data is that the MR-dependent increase in energy intake is dependent on a coordinated MR-dependent increase in EE. Arguing against such a mechanism are the effects of dietary leucine deprivation, which results in food aversion despite a significant increase in EE (53–55). Perhaps the absence of FGF21 heightens the central perception of reduced methionine such that it is interpreted as methionine deprivation with respect to energy intake. Cell type–specific deletion of FGF21 signaling in CNS sites involved in essential amino acid sensing would be one approach to test this possibility.

The previously reported activation of NRF2-sensitive and ATF4-sensitive genes by MR and the downregulation of hepatic lipogenic genes and tissue triglycerides by MR (1,15) were not compromised in *Fgf21*$^{-/-}$ mice, establishing that FGF21 is not the mediator of these effects of MR in the liver. We previously showed that addition of small amounts of cysteine to the MR diet fully reversed the transcriptional activation of hepatic *Fgf21* by MR (13) but that the downregulation of *Scd1* was unaffected. However, the activation of NRF2- and ATF4-sensitive genes by MR in the liver was reversed by adding cysteine back to the diet (13), supporting our view that these transcriptional effects of MR are directly linked to methionine/cysteine sensing in the liver and are not secondary to FGF21. However, MR was unable to reduce serum triglyceride in *Fgf21*$^{-/-}$ mice, suggesting a requirement for FGF21 for this effect. We believe this effect is associated with FGF21-dependent remodeling of BAT and WAT and the enhanced clearance of serum triglycerides by enhanced thermogenesis (56). Recent work showed that FGF21 lowered plasma triglycerides by accelerating lipoprotein catabolism in WAT and BAT (57). Thus, the failure of MR to decrease serum triglycerides in *Fgf21*$^{-/-}$ mice was due to the inability of MR to enhance thermogenic activity in BAT and WAT in the absence of FGF21. It will be important to test this hypothesis experimentally using tracer-based methods to measure fatty acid uptake and utilization among tissues. On the basis of the present findings, we propose that FGF21 is a key mediator linking sensing of the reduction of dietary methionine in the liver to its effects on energy balance, insulin sensitivity, and adipose tissue remodeling, but not its transcriptional effects in the liver.

Acknowledgments. The authors thank Kelly Dille, Kodi Bethay, and Jaroslaw Staszkiewicz from the corresponding author's laboratory at Pennington Biomedical Research Center for excellent technical support and Dr. Chris Morrison of the Pennington Biomedical Research Center for helpful discussions during the preparation of the manuscript. The authors thank Cindi Tramonte (Pennington Biomedical Research Center) for administrative support.

Funding. D.W. is supported by a National Institute of Diabetes and Digestive and Kidney Diseases National Institutes of Health (NIH) National Research Service Award (NIH NRSA 1-F32-DK-098918). L.A.F. is supported by an American Diabetes Association mentor-based postdoctoral fellowship (7-13-MI-05). This work was partly supported by American Diabetes Association grant 1-12-BS-58 (T.W.G.), National Institute of Diabetes and Digestive and Kidney Diseases grant NIH R01-DK-096311 (T.W.G.), and the Mouse Metabolic Phenotyping Center Consortium (NIH U24-DK-059637). This work also made use of the Genomics and Cell Biology & Bioimaging core facilities supported by National Institute of General Medical Sciences grant NIH 3P30 GM118430 (T.W.G.). This research project used the Transgenic and Animal Phenotyping core facilities that are supported in part by the National Institute of Diabetes and Digestive and Kidney Diseases Nutrition Obesity Research Centers grant NIH 3P30-DK-072476.

Duality of Interest. No potential conflicts of interest relevant to this article were reported.

Author Contributions. D.W., L.A.F., and T.W.G. contributed to the writing and editing of the manuscript. D.W., L.A.F., K.P.S., and A.P. conducted the animal experiments, the in vitro analysis, and the associated Western blots, mRNA, and metabolite measurements. L.A.F. and T.W.G. and analyzed the data used to produce illustrations. D.H.B. conducted the imaging analysis. T.W.G. is the guarantor of this work and, as such, had full access to all the data in the study and takes responsibility for the integrity of the data and the accuracy of the data analysis.

References

1. Hasek BE, Boudreau A, Shin J, et al. Remodeling the integration of lipid metabolism between liver and adipose tissue by dietary methionine restriction in rats. Diabetes 2013;62:3362–3372

2. Hasek BE, Stewart LK, Henagan TM, et al. Dietary methionine restriction enhances metabolic flexibility and increases uncoupled respiration in both fed and fasted states. Am J Physiol Regul Integr Comp Physiol 2010;299:R728–R739

3. Malloy VL, Krajcik RA, Bailey SJ, Hristopoulos G, Plummer JD, Orentreich N. Methionine restriction decreases visceral fat mass and preserves insulin action in aging male Fischer 344 rats independent of energy restriction. Aging Cell 2006;5:305–314

4. Wanders D, Burk DH, Cortez CC, et al. UCP1 is an essential mediator of the effects of methionine restriction on energy balance but not insulin sensitivity. FASEB J 2015;29:2603–2615

5. Stone KP, Wanders D, Orgeron M, Cortez CC, Gettys TW. Mechanisms of increased in vivo insulin sensitivity by dietary methionine restriction in mice. Diabetes 2014;63:3721–3733

6. Kimball SR. Regulation of global and specific mRNA translation by amino acids. J Nutr 2002;132:883–886

7. Kobayashi H, Børsheim E, Anthony TG, et al. Reduced amino acid availability inhibits muscle protein synthesis and decreases activity of initiation factor eIF2B. Am J Physiol Endocrinol Metab 2003;284:E488–E498

8. Zhang P, McGrath BC, Reinert J, et al. The GCN2 eIF2alpha kinase is required for adaptation to amino acid deprivation in mice. Mol Cell Biol 2002;22:6681–6688

9. Gietzen DW, Ross CM, Hao S, Sharp JW. Phosphorylation of eIF2alpha is involved in the signaling of indispensable amino acid deficiency in the anterior piriform cortex of the brain in rats. J Nutr 2004;134:717–723

10. Deval C, Chaveroux C, Maurin AC, et al. Amino acid limitation regulates the expression of genes involved in several specific biological processes through GCN2-dependent and GCN2-independent pathways. FEBS J 2009;276:707–718

11. Siu F, Bain PJ, LeBlanc-Chaffin R, Chen H, Kilberg MS. ATF4 is a mediator of the nutrient-sensing response pathway that activates the human asparagine synthetase gene. J Biol Chem 2002;277:24120–24127

12. Pan Y, Chen H, Siu F, Kilberg MS. Amino acid deprivation and endoplasmic reticulum stress induce expression of multiple activating transcription factor-3

mRNA species that, when overexpressed in HepG2 cells, modulate transcription by the human asparagine synthetase promoter. J Biol Chem 2003;278:38402–38412
13. Wanders D, Stone KP, Forney LA, et al. Role of GCN2-independent signaling through a non-canonical PERK/NRF2 pathway in the physiological responses to dietary methionine restriction. Diabetes 2016;65:1499–1510
14. Plaisance EP, Henagan TM, Echlin H, et al. Role of β-adrenergic receptors in the hyperphagic and hypermetabolic responses to dietary methionine restriction. Am J Physiol Regul Integr Comp Physiol 2010;299:R740–R750
15. Stone KP, Wanders D, Calderon LF, Spurgin SB, Scherer PE, Gettys TW. Compromised responses to dietary methionine restriction in adipose tissue but not liver of ob/ob mice. Obesity (Silver Spring) 2015;23:1836–1844
16. Coskun T, Bina HA, Schneider MA, et al. Fibroblast growth factor 21 corrects obesity in mice. Endocrinology 2008;149:6018–6027
17. Holland WL, Adams AC, Brozinick JT, et al. An FGF21-adiponectin-ceramide axis controls energy expenditure and insulin action in mice. Cell Metab 2013;17:790–797
18. Kharitonenkov A, Shiyanova TL, Koester A, et al. FGF-21 as a novel metabolic regulator. J Clin Invest 2005;115:1627–1635
19. Adams AC, Coskun T, Rovira AR, et al. Fundamentals of FGF19 & FGF21 action in vitro and in vivo. PLoS One 2012;7:e38438
20. Xu J, Stanislaus S, Chinookoswong N, et al. Acute glucose-lowering and insulin-sensitizing action of FGF21 in insulin-resistant mouse models–association with liver and adipose tissue effects. Am J Physiol Endocrinol Metab 2009;297: E1105–E1114
21. Bookout AL, de Groot MH, Owen BM, et al. FGF21 regulates metabolism and circadian behavior by acting on the nervous system. Nat Med 2013;19:1147–1152
22. Xu J, Lloyd DJ, Hale C, et al. Fibroblast growth factor 21 reverses hepatic steatosis, increases energy expenditure, and improves insulin sensitivity in diet-induced obese mice. Diabetes 2009;58:250–259
23. Angelin B, Larsson TE, Rudling M. Circulating fibroblast growth factors as metabolic regulators–a critical appraisal. Cell Metab 2012;16:693–705
24. Ghosh S, Wanders D, Stone KP, Van NT, Cortez CC, Gettys TW. A systems biology analysis of the unique and overlapping transcriptional responses to caloric restriction and dietary methionine restriction in rats. FASEB J 2014;28:2577–2590
25. Ayala JE, Bracy DP, McGuinness OP, Wasserman DH. Considerations in the design of hyperinsulinemic-euglycemic clamps in the conscious mouse. Diabetes 2006;55:390–397
26. Wanders D, Stone KP, Dille K, Simon J, Pierse A, Gettys TW. Metabolic responses to dietary leucine restriction involve remodeling of adipose tissue and enhanced hepatic insulin signaling. Biofactors 2015;41:391–402
27. Patil YN, Dille KN, Burk DH, Cortez CC, Gettys TW. Cellular and molecular remodeling of inguinal adipose tissue mitochondria by dietary methionine restriction. J Nutr Biochem 2015;26:1235–1247
28. Orentreich N, Matias JR, DeFelice A, Zimmerman JA. Low methionine ingestion by rats extends life span. J Nutr 1993;123:269–274
29. Zimmerman JA, Malloy V, Krajcik R, Orentreich N. Nutritional control of aging. Exp Gerontol 2003;38:47–52
30. Miller RA, Buehner G, Chang Y, Harper JM, Sigler R, Smith-Wheelock M. Methionine-deficient diet extends mouse lifespan, slows immune and lens aging, alters glucose, T4, IGF-I and insulin levels, and increases hepatocyte MIF levels and stress resistance. Aging Cell 2005;4:119–125
31. Sun L, Sadighi Akha AA, Miller RA, Harper JM. Life-span extension in mice by preweaning food restriction and by methionine restriction in middle age. J Gerontol A Biol Sci Med Sci 2009;64:711–722
32. Richie JP Jr, Leutzinger Y, Parthasarathy S, Malloy V, Orentreich N, Zimmerman JA. Methionine restriction increases blood glutathione and longevity in F344 rats. FASEB J 1994;8:1302–1307
33. Lees EK, Król E, Grant L, et al. Methionine restriction restores a younger metabolic phenotype in adult mice with alterations in fibroblast growth factor 21. Aging Cell 2014;13:817–827
34. Ables GP, Perrone CE, Orentreich D, Orentreich N. Methionine-restricted C57BL/6J mice are resistant to diet-induced obesity and insulin resistance but have low bone density. PLoS One 2012;7:e51357
35. Lin Z, Tian H, Lam KS, et al. Adiponectin mediates the metabolic effects of FGF21 on glucose homeostasis and insulin sensitivity in mice. Cell Metab 2013; 17:779–789
36. Fisher FM, Kleiner S, Douris N, et al. FGF21 regulates PGC-1α and browning of white adipose tissues in adaptive thermogenesis. Genes Dev 2012; 26:271–281
37. Emanuelli B, Vienberg SG, Smyth G, et al. Interplay between FGF21 and insulin action in the liver regulates metabolism. J Clin Invest 2014;124:515–527
38. Véniant MM, Sivits G, Helmering J, et al. Pharmacologic effects of FGF21 are independent of the "browning" of white adipose tissue. Cell Metab 2015;21: 731–738
39. Samms RJ, Smith DP, Cheng CC, et al. Discrete aspects of FGF21 in vivo pharmacology do not require UCP1. Cell Reports 2015;11:991–999
40. Ding X, Boney-Montoya J, Owen BM, et al. βKlotho is required for fibroblast growth factor 21 effects on growth and metabolism. Cell Metab 2012;16:387–393
41. Adams AC, Yang C, Coskun T, et al. The breadth of FGF21's metabolic actions are governed by FGFR1 in adipose tissue. Mol Metab 2012;2:31–37
42. Camacho RC, Zafian PT, Achanfuo-Yeboah J, Manibusan A, Berger JP. Pegylated Fgf21 rapidly normalizes insulin-stimulated glucose utilization in diet-induced insulin resistant mice. Eur J Pharmacol 2013;715:41–45
43. Bröer A, Juelich T, Vanslambrouck JM, et al. Impaired nutrient signaling and body weight control in a Na+ neutral amino acid cotransporter (Slc6a19)-deficient mouse. J Biol Chem 2011;286:26638–26651
44. Jiang Y, Rose AJ, Sijmonsma TP, et al. Mice lacking neutral amino acid transporter B(0)AT1 (Slc6a19) have elevated levels of FGF21 and GLP-1 and improved glycaemic control. Mol Metab 2015;4:406–417
45. Markan KR, Naber MC, Ameka MK, et al. Circulating FGF21 is liver derived and enhances glucose uptake during refeeding and overfeeding. Diabetes 2014; 63:4057–4063
46. Owen BM, Ding X, Morgan DA, et al. FGF21 acts centrally to induce sympathetic nerve activity, energy expenditure, and weight loss. Cell Metab 2014;20:670–677
47. Douris N, Stevanovic DM, Fisher FM, et al. Central fibroblast growth factor 21 browns white fat via sympathetic action in male mice. Endocrinology 2015; 156:2470–2481
48. Badman MK, Koester A, Flier JS, Kharitonenkov A, Maratos-Flier E. Fibroblast growth factor 21-deficient mice demonstrate impaired adaptation to ketosis. Endocrinology 2009;150:4931–4940
49. Camporez JP, Asrih M, Zhang D, et al. Hepatic insulin resistance and increased hepatic glucose production in mice lacking Fgf21. J Endocrinol 2015; 226:207–217
50. Fisher FM, Chui PC, Antonellis PJ, et al. Obesity is a fibroblast growth factor 21 (FGF21)-resistant state. Diabetes 2010;59:2781–2789
51. Singhal G, Fisher FM, Chee MJ, et al. Fibroblast growth factor 21 (FGF21) protects against high fat diet induced inflammation and islet hyperplasia in pancreas. PLoS One 2016;11:e0148252
52. Laeger T, Henagan TM, Albarado DC, et al. FGF21 is an endocrine signal of protein restriction. J Clin Invest 2014;124:3913–3922
53. Guo F, Cavener DR. The GCN2 eIF2alpha kinase regulates fatty-acid homeostasis in the liver during deprivation of an essential amino acid. Cell Metab 2007;5:103–114
54. Cheng Y, Zhang Q, Meng Q, et al. Leucine deprivation stimulates fat loss via increasing CRH expression in the hypothalamus and activating the sympathetic nervous system. Mol Endocrinol 2011;25:1624–1635
55. Cheng Y, Meng Q, Wang C, et al. Leucine deprivation decreases fat mass by stimulation of lipolysis in white adipose tissue and upregulation of uncoupling protein 1 (UCP1) in brown adipose tissue. Diabetes 2010;59:17–25
56. Bartelt A, Bruns OT, Reimer R, et al. Brown adipose tissue activity controls triglyceride clearance. Nat Med 2011;17:200–205
57. Schlein C, Talukdar S, Heine M, et al. FGF21 lowers plasma triglycerides by accelerating lipoprotein catabolism in white and brown adipose tissues. Cell Metab 2016;23:441–453